

**NANO EXPRESS**

**Open Access**



# Red-Shift Effect and Sensitive Responsivity of MoS<sub>2</sub>/ZnO Flexible Photodetectors

Yu-Jen Hsiao<sup>1</sup>, Te-Hua Fang<sup>2\*</sup>, Liang-Wen Ji<sup>3</sup> and Bo-Yi Yang<sup>2</sup>

## Abstract

The optoelectronic characteristics of molybdenum disulfide (MoS<sub>2</sub>)/ZnO flexible photodetectors are investigated. A red-shift effect and improved photocurrent properties of the flexible devices are demonstrated. MoS<sub>2</sub> doping improved the photocurrent properties and conductivity. The photocurrent/dark current ratios of pure ZnO and MoS<sub>2</sub>/ZnO flexible photodetectors were 10<sup>3</sup> and 10<sup>4</sup>, respectively. The responsivity of MoS<sub>2</sub>/ZnO increased, and the wavelength was red-shifted.

**Keywords:** MoS<sub>2</sub>, Photodetectors, Photo-induced response, Flexible

## Background

Molybdenum disulfide (MoS<sub>2</sub>) is a promising candidate for optoelectronic sensors because of its unique semi-conducting channel when used as a phototransistor [1]. MoS<sub>2</sub> phototransistors have recently been integrated with conventional semiconductor circuitry [2]. Bulk MoS<sub>2</sub> is an indirect-gap semiconductor with a bandgap of 1.2 eV [3], whereas a single-layer MoS<sub>2</sub> is a direct-gap semiconductor with a bandgap of 1.8 eV [4]. The photodetector (PD) has a broad spectral range, with photocurrent that monotonously increases as the wavelength of incident light is decreased from 680 to 400 nm. Two-dimensional and single-layer ultrasensitive MoS<sub>2</sub> PDs have a photoresponsivity that is 10<sup>6</sup> better than that of the first graphene PDs (~0.5 mA W<sup>-1</sup>) [5]. In addition, a high-performance complementary inverter and selective gas sensing based on MoS<sub>2</sub> field-effect transistors was studied [6–8].

There are various ways of synthesizing MoS<sub>2</sub> nanostructures including electrochemical/chemical synthesis [9], laser ablation [10], solution-based exfoliation [11], and chemical vapor deposition (CVD) [12]. Another method, the rapid vibro-milling technique, was employed for investigating the potentiality of obtaining nano-sized powders. MoS<sub>2</sub> nanoparticles obtained using vibro-milling, which can be applied at an industrial scale, have good solubility and biocompatibility.

However, few applications of MoS<sub>2</sub> synthesized by rapid vibro-milling have been reported. The rapid vibro-milling process was employed for investigating its potential for obtaining nanometer-sized powders [13]. The electro-optical properties of ZnO compounds have been studied extensively [14]. To our knowledge, MoS<sub>2</sub>/ZnO films have not been thoroughly investigated, which is the motivation for this research. The morphology and photoresponsivity properties of the MoS<sub>2</sub> nanocrystals on ZnO film are studied and discussed.

## Methods

Nanocrystalline MoS<sub>2</sub> (from Alfa Aesar, 325 mesh, 99 %) was prepared using a high-energy ball-milling method. MoS<sub>2</sub> was milled in ceramic milling vials (zirconia) using zirconia balls for 10, 20, and 40 h. The ball-to-powder weight ratio was 2:1 to produce at least 2 g of nanopowder. The mechanical milling was performed in a horizontal oscillatory mill (Retsch, PM 400) operating at 25 Hz. The as-synthesized materials were characterized by X-ray diffraction (XRD, Rigaku Dmax-33). The morphology and microstructure were examined using atomic force microscopy (AFM, Bruker) and transmission electron microscopy (TEM, Hitachi HF-2000).

In this work, MoS<sub>2</sub>/ZnO was used to fabricate metal-semiconductor-metal (MSM) ultraviolet (UV) PDs, as shown in Fig. 1a. ZnO thin films were deposited on polyethylene naphthalate (PEN) substrates using radio frequency (RF) magnetron sputtering. During growth, the working pressure of the chamber was about 5 × 10<sup>-2</sup> Torr,

\* Correspondence: fang.tehua@msa.hinet.net

<sup>2</sup>Department of Mechanical Engineering, National Kaohsiung University of Applied Sciences, Kaohsiung 807, Taiwan

Full list of author information is available at the end of the article

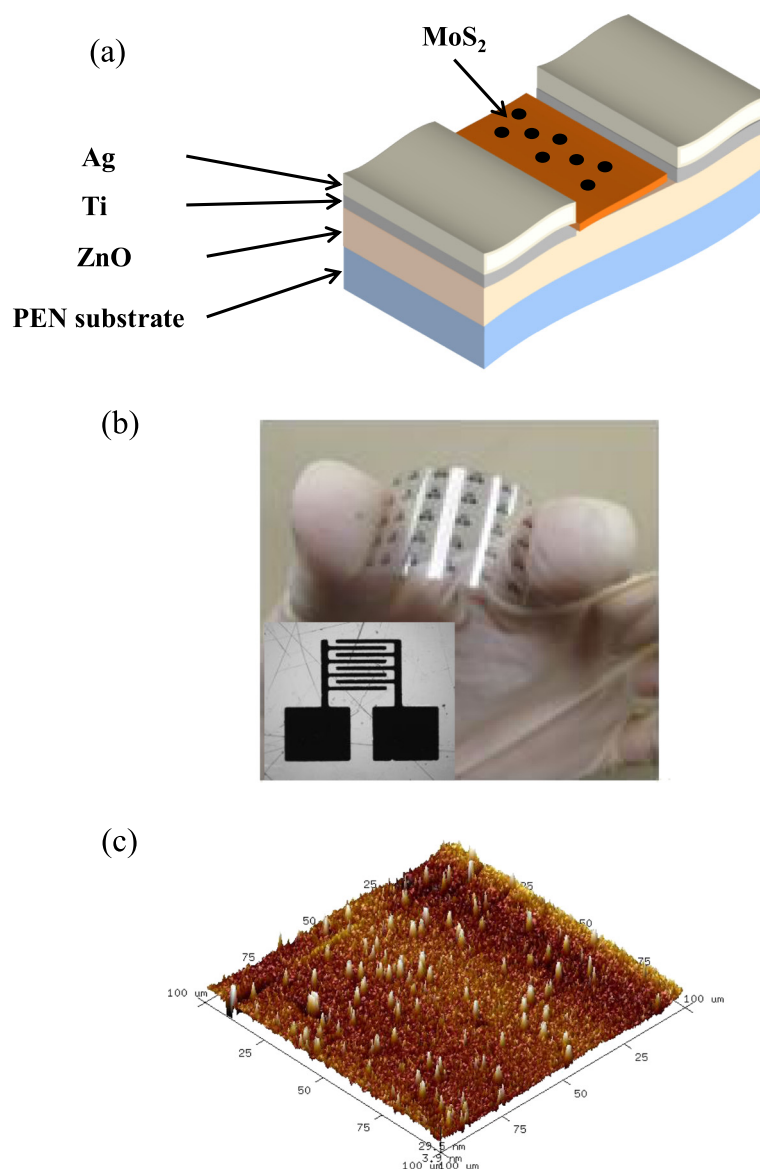


**Fig. 1** **a** Schematic diagram of flexible MoS<sub>2</sub>/ZnO PD. **b** Optical image of MoS<sub>2</sub>/ZnO PD fabricated on PEN substrate. *Inset* shows electrode pattern structure. **c** AFM image of 5 wt% MoS<sub>2</sub> nanocrystal coating on ZnO/PEN substrate

the RF power was 250 W, and the gas mixing ratio (Ar/O<sub>2</sub>) was 10:1. The thickness of the ZnO film was 100 nm. Ag/Ti electrodes were used to provide ohmic contact on the ZnO film. They were deposited using the electron beam evaporation method. The fingers of the Ag contact electrodes had a width of 20 μm, a length of 250 μm, and a space of 20 μm. In 10 cm<sup>3</sup> of alcohol, 0, 0.1, and 0.2 g of MoS<sub>2</sub> nanopowder were dissolved, respectively. The PD materials of MoS<sub>2</sub> were spin-coated with a rotation speed of 300 RPM in the air. The photocurrent, dark current, and responsivity of the PDs were measured using an HP4156C semiconductor parameter analyzer. The spectral response of the PDs was measured with a light source which employed a 300-W

xenon lamp as the light source and a monochromator covering the range of 300–700 nm.

## Results and Discussion

Figure 1b shows an optical image of the flexible PDs with MoS<sub>2</sub> coated on the ZnO/PEN substrate. The PDs exhibited a transmission of above 80 % and high bending strength. The bending curvature radius was larger than 10 mm. The Ag electrode pattern is shown in the inset of Fig. 1b. The interdigital electrodes have eight fingers with a fixed length of 2000 μm and a width of 50 μm. The spin-coated 5 wt% MoS<sub>2</sub> nanocrystals on the ZnO/PEN substrate were also characterized using AFM to better understand the morphological properties with a

large area of  $100 \times 100 \mu\text{m}$ , as shown in Fig. 1c. The pure ZnO film has a root-mean-square (rms) roughness of 13.2 nm, and the spin-coated  $\text{MoS}_2$  on the ZnO film has that of 84.9 nm. In this study, the particle size of  $\text{MoS}_2$  was around 20–50 nm. During the spin-coating of  $\text{MoS}_2$ , the nanocrystals had a uniform morphology and monodispersity. They were deposited on the ZnO/PEN substrate due to the gravitational force, causing the high roughness on the ZnO/PEN substrate.

$\text{MoS}_2$  exhibits the characteristic peaks of a polycrystal structure in the XRD analysis, as shown in Fig. 2a. The XRD patterns also have a strong (002) peak, with a preferred orientation at  $2\theta = 10.47^\circ$ . No secondary phases were detected for the pure  $\text{MoS}_2$  samples. Nanocrystalline  $\text{MoS}_2$  was obtained using high-energy ball-milling. The full width at half maximum of the diffraction peak

is rather small, which indicates that the film crystallinity is fairly good for the pristine  $\text{MoS}_2$  powder. The average grain size was determined by the line broadening of XRD patterns for various milling times. Many hours of milling were sufficient to produce nanocrystalline powders.

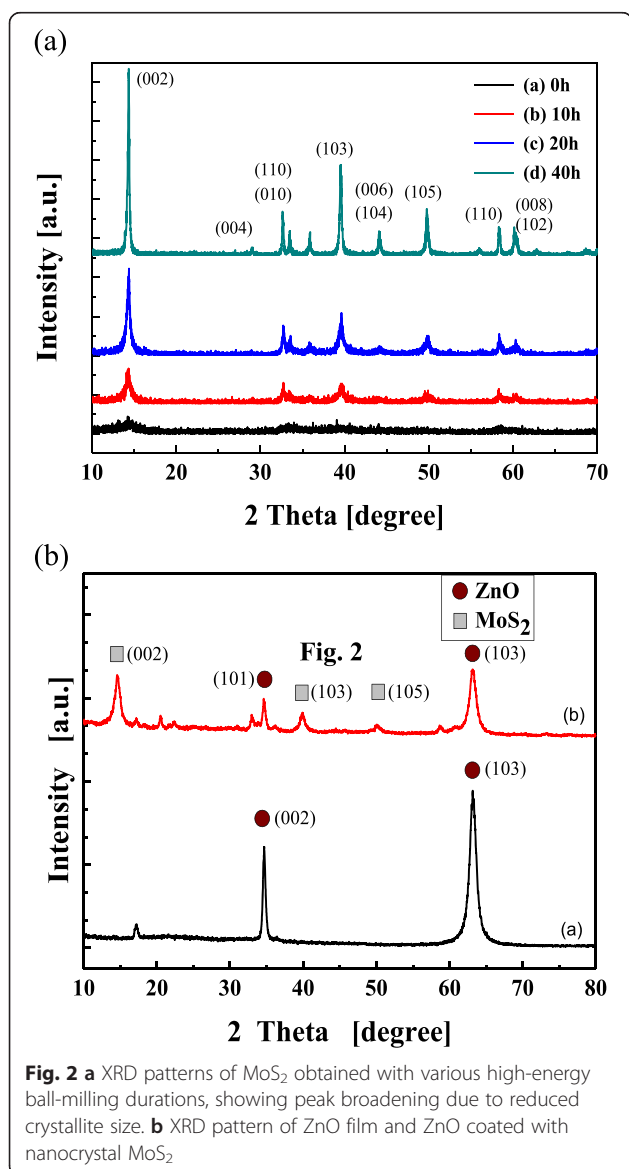
The average grain sizes were determined from XRD according to Scherrer's equation [15]:

$$D = \frac{k\lambda}{\beta \cos\theta} \quad (1)$$

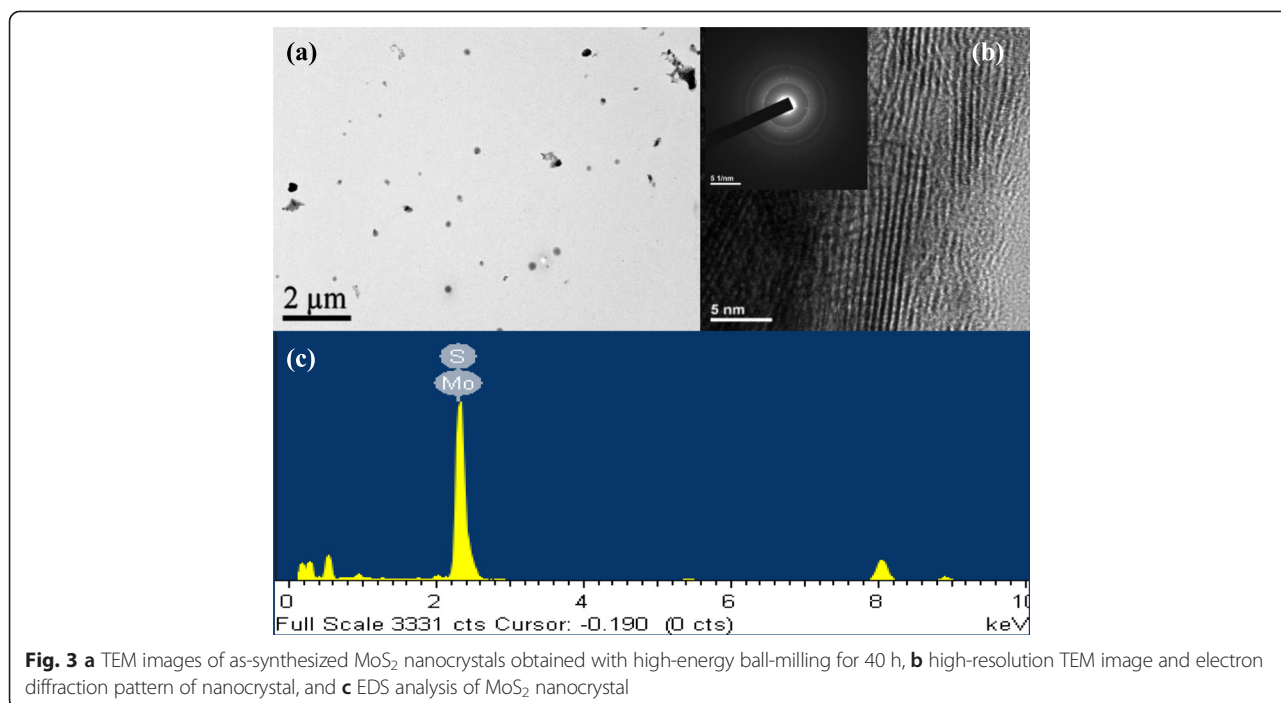
where  $D$  is the average grain size,  $k$  is a constant (equal to 0.89),  $\lambda$  is the X-ray wavelength (equal to 0.1542 nm),  $\theta$  is the (002) peak angle, and  $\beta$  is half the peak width. The average grain size of powders milled for 20 h was 28.4 nm. The line broadening of the nanocrystalline samples is due to the small grain size and strain-induced response [16]. Figure 2b shows the XRD patterns of ZnO and ZnO films with 5 wt%  $\text{MoS}_2$  (~28 nm) coating layer. A (002) peak at  $34.5^\circ$  along with a strong (103) peak was observed for the ZnO thin films, indicating the polycrystalline nature of the thin films. The peak position of ZnO remains almost unchanged because the bottom ZnO layers were controlled to have a thickness of 100 nm. Therefore, the nanocrystalline  $\text{MoS}_2$  can be observed on the ZnO thin film by grazing incidence XRD.

Figure 3a shows a low-magnification TEM image. Spherical nanocrystals can be clearly observed. The diameter of the nanocrystals was about 20–50 nm. Figure 3b shows a high-resolution TEM image, indicating the periodic atom arrangement of the  $\text{MoS}_2$  nanosheets at a selected location. The interplanar distances of the crystal fringes are about 5.08 Å, corresponding to the spacing  $d$ -[100] of hexagonal  $\text{MoS}_2$  (JCPDS card no. 77-1716). A polycrystalline phase was present in the  $\text{MoS}_2$  matrix. The well-defined selected area electron diffraction (SAED) pattern clearly shows the diffraction spots in the inset of Fig. 3b. The energy-dispersive X-ray spectroscopy (EDS) line profiles indicate that the nanocrystal consists of Mo and S as shown in Fig. 3c. The signals were generated by the nanobeam incident to the nanocrystal  $\text{MoS}_2$ .

Figure 4 shows the current-voltage ( $I$ - $V$ ) characteristics of the PDs with different  $\text{MoS}_2$  layers under dark and illumination conditions. The measurements were conducted at 5-V bias and 340-nm illumination. The results show that the light current of the photodetectors with  $\text{MoS}_2$  layers was enhanced. The highest photocurrent was obtained for the device with a 5 wt%  $\text{MoS}_2$  layer. The photocurrent to dark current contrast ratios of the 0, 1, and 5 wt%  $\text{MoS}_2$  PDs biased at 5 V were 8840, 13,100, and 17,800, respectively.  $\text{MoS}_2$  thus increased optical absorption. The dark current of the  $\text{MoS}_2$  film was very small. This may be due to the low background carrier concentration. The photo-generated holes recombined



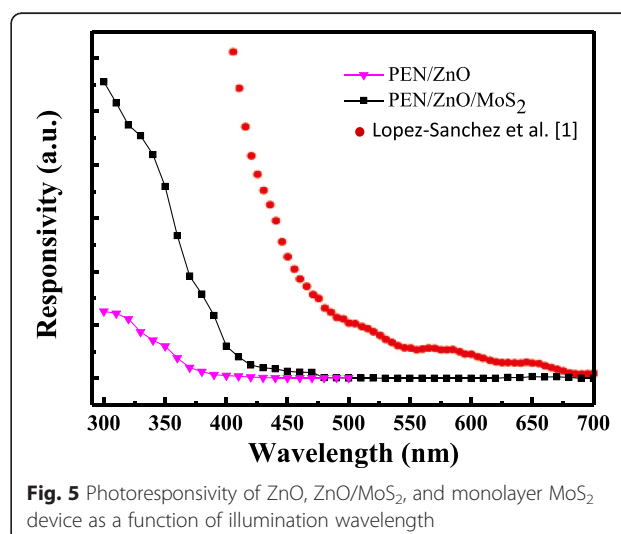
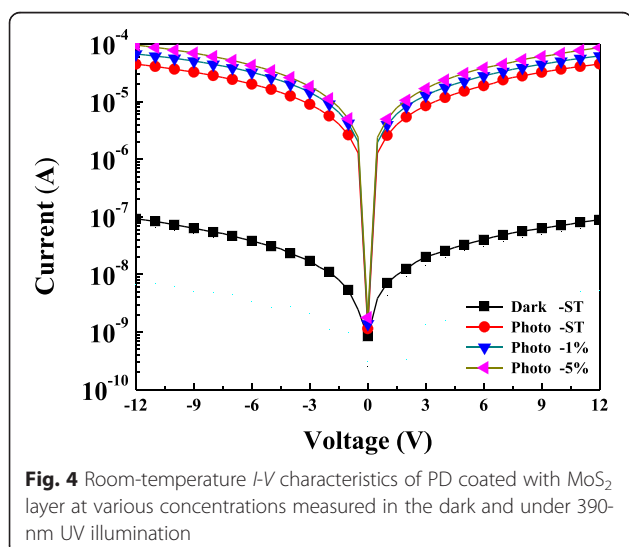
**Fig. 2** **a** XRD patterns of  $\text{MoS}_2$  obtained with various high-energy ball-milling durations, showing peak broadening due to reduced crystallite size. **b** XRD pattern of ZnO film and ZnO coated with nanocrystal  $\text{MoS}_2$



with the surface-adsorbed oxygen ions. The results show that hole and electron pairs were generated when UV light illuminated the ZnO layer. PD devices based on MoS<sub>2</sub> thus exhibit a very high photoresponsivity [1, 17]. The high performance can be ascribed to the straight electron transport path offered by nanocrystalline MoS<sub>2</sub> powders. The MoS<sub>2</sub> nanopowders have a high surface-to-volume ratio. A heterojunction forms at the interface between ZnO and MoS<sub>2</sub> nanopowders.

Figure 5 shows the photoresponsivity of pure ZnO and 5 wt% MoS<sub>2</sub>/ZnO PDs in the UV-to-visible light region. The device with MoS<sub>2</sub> nanopowders shows a red shift

(from 360 to 420 nm) and increased photocurrent. The photoresponsivity of the composite MoS<sub>2</sub>/ZnO device as a function of illumination wavelength was measured. The response increased as the illumination wavelength was reduced from 420 to 300 nm. The higher responsivity of the 5 wt% MoS<sub>2</sub>/ZnO PD compared with that of ZnO is attributed to the improved carrier transport and collection efficiency [18]. The adsorbates on the MoS<sub>2</sub> surface or at the MoS<sub>2</sub>/ZnO interface affect not only the carrier transport behaviors but also the photoelectrical responses [19]. The optical properties of nanocrystalline MoS<sub>2</sub> have been measured by UV/VIS



absorption spectroscopy technique. The optical absorption spectrum of MoS<sub>2</sub> nanocrystallines shows a minimum optical absorption feature of about 400 nm and strong rising absorption edge shifts towards the UV region. Therefore, the prepared MoS<sub>2</sub>/ZnO MSM photodetectors generated photoresponse between 300 and 420 nm UV range and diminishing photoresponse at the visible range. A good agreement is observed between the MoS<sub>2</sub> nanocrystalline absorption characteristics and the photoresponsivity data. Lopez-Sanchez et al. demonstrated ultrasensitive monolayer MoS<sub>2</sub> phototransistors with improved device mobility and ON current [1]. A thin film of MoS<sub>2</sub> nanocrystals has also been demonstrated through laser ablation that it could be used as a material for the fabrication of UV PDs [17]. This flexible MoS<sub>2</sub>/ZnO optoelectronic devices could be used in fields of low-light imaging sensors.

## Conclusions

MoS<sub>2</sub> nanopowder was deposited on flexible devices using high-energy ball-milling method. Flexible ZnO and MoS<sub>2</sub>/ZnO MSM PDs were investigated. The results show that the photocurrent/dark current ratios of pure ZnO and MoS<sub>2</sub>/ZnO flexible PDs were 10<sup>3</sup> and 10<sup>4</sup>, respectively. The responsivity increased and the wavelength was red-shifted when a 5 wt% MoS<sub>2</sub> layer was used. There was a significant improvement in the photo-induced properties.

## Competing interests

The authors declare that they have no competing interests.

## Authors' Contributions

YJ and BY carried out the synthesis and characterization of the samples, analyzed the results, and wrote the first draft of the manuscript. TH participated in the design, preparation, and discussion of this study. LW contributed ideas for the growth of the samples and revised the manuscript. All authors read and approved the final manuscript.

## Acknowledgements

This work was partially supported by the Ministry of Science and Technology of Taiwan under grants MOST 103-2221-E-151-001-MY3 and MOST 103-2221-E-151-007-MY3.

## Author details

<sup>1</sup>National Nano Device Laboratories, National Applied Research Laboratories, Tainan 741, Taiwan. <sup>2</sup>Department of Mechanical Engineering, National Kaohsiung University of Applied Sciences, Kaohsiung 807, Taiwan. <sup>3</sup>Institute of Electro-Optical and Materials Science, National Formosa University, Yunlin 632, Taiwan.

Received: 7 October 2015 Accepted: 11 November 2015

Published online: 16 November 2015

## References

- Lopez-Sanchez O, Lembke D, Kayci M, Radenovic A, Kis A (2013) Ultrasensitive photodetectors based on monolayer MoS<sub>2</sub>. *Nat Nanotech* 8:497
- Gu W, Shen J, Ma X (2014) Fabrication and electrical properties of MoS<sub>2</sub> nanodisc-based back-gated field effect transistors. *Nanoscale Res Lett* 9:100
- Kam KK, Parkinson BA (1982) Detailed photocurrent spectroscopy of the semiconducting group VIb transition metal dichalcogenides. *J Phys Chem* 86:463
- Mak KF, Lee C, Hone J, Shan J, Heinz TF (2010) Atomically thin MoS<sub>2</sub>: a new direct-gap semiconductor. *Phys Rev Lett* 105:136805
- Xia F, Mueller T, Lin YM, Valdes-Garcia A, Avouris P (2009) Ultrafast graphene photodetector. *Nat Nanotech* 4:839
- Cho AJ, Park KC, Kwon YJ (2015) A high-performance complementary inverter based on transition metal dichalcogenide field-effect transistors. *Nanoscale Res Lett* 10:115
- Yin Z, Li H, Jiang L, Shi Y, Sun Y, Lu G, Zhang Q, Chen X, Zhang H (2012) Single-layer MoS<sub>2</sub> phototransistors. *ACS Nano* 6:74
- Mueller T, Xia F, Avouris P (2010) Graphene photodetectors for high-speed optical communications. *Nat Photon* 4:297
- Li Q, Newberg JT, Walther EC, Hemminger JC, Penner RM (2004) Polycrystalline molybdenum disulfide (2H-MoS<sub>2</sub>) nano- and microribbons by electrochemical/chemical synthesis. *Nano Lett* 4:277
- Wu H, Yang R, Song B, Han Q, Li J, Zhang Y, Fang Y, Tenne R, Wang C (2011) Biocompatible inorganic fullerene-like molybdenum disulfide nanoparticles produced by pulsed laser ablation in water. *ACS Nano* 5:1276
- Coleman JN, Lotya M, O'Neill A, Bergin SD, King PJ, Khan U, Young K, Gaucher A, De S, Smith RJ, Shvets IV, Arora SK, Stanton G, Kim HY, Lee K, Kim GT, Duesberg GS, Hallam T, Boland JJ, Wang JJ, Donegan TF, Grunlan JC, Moriarty G, Shmeliov A, Nicholls RJ, Perkins JM, Grieveson EM, Theuwissen K, McComb DW, Nellist PD, Nicolosi V (2011) Two-dimensional nanosheets produced by liquid exfoliation of layered materials. *Science* 331:568
- Zhan Y, Liu Z, Najmaei S, Ajayan PM, Lou J (2012) Large-area vapor-phase growth and characterization of MoS<sub>2</sub> atomic layers on a SiO<sub>2</sub> substrate. *Small* 28:966
- Hsiao YJ, Chai YL, Ji LW, Fang TH, Meen TH, Tsai JK, Chen KL, Prior SD (2012) Optical characteristics of LiZnVO<sub>4</sub> green phosphor at low temperature preparation. *Mater Lett* 70:163
- Peng SM, Su YK, Ji W, Young SJ, Tsai CN, Hong JH, Chen ZS, Wu CZ (2011) Transparent ZnO nanowire-network ultraviolet photosensor. *IEEE Trans Electron Devices* 58:2036
- Hsiao YJ, Meen TH, Ji LW, Tsai JK, Wu YS, Huang CJ (2013) Preparation of ZnS microdisks using chemical bath deposition and ZnS/p-Si heterojunction solar cells. *J Phys Chem Solids* 74:1403
- Willimason GK, Hall WH (1953) X-ray line broadening from fcc aluminium and wolfram. *Acta Metall* 1:22
- Xie Y, Wei L, Li Q, Chen Y, Yan S, Jiao J, Liu G, Mei L (2014) High-performance self-powered UV photodetectors based on TiO<sub>2</sub> nano-branched arrays. *Nanotechnol* 25:075202
- Alkis S, Öztaş T, Aygün LE, Bozkurt F, Okyay AK, Ortaç B (2012) Thin film MoS<sub>2</sub> nanocrystal based ultraviolet photodetector. *Opt Express* 20:21815
- Choi W, Cho MY, Konar A, Lee JH, Cha GB, Hong SC, Kim S, Kim J, Jena D, Joo J, Kim S (2012) High-detectivity multilayer MoS<sub>2</sub> phototransistors with spectral response from ultraviolet to infrared. *Adv Mater* 24:5832

Submit your manuscript to a SpringerOpen<sup>®</sup> journal and benefit from:

- Convenient online submission
- Rigorous peer review
- Immediate publication on acceptance
- Open access: articles freely available online
- High visibility within the field
- Retaining the copyright to your article

Submit your next manuscript at ► [springeropen.com](http://springeropen.com)